

## Study on low melting nanocrystalline Sn-0.7Cu solder alloy

I. Narasimha Murthy<sup>1</sup>, K. Sivaprasad<sup>2</sup> and J. Babu Rao\*<sup>1</sup>

<sup>1</sup>Department of Metallurgical Engineering, Andhra University College of Engineering (A) Viskhapatnam-530 003, INDIA

<sup>2</sup>Department. of Metallurgical and Materials Engineering, National Institute of Technology, Trichy-620 015, INDIA

\*Corresponding Author's e-mail: baburaojinugu@yahoo.com, Tel +91-9848431073

### Abstract

Research was conducted to build up the minimal cost nano-crystalline *Pb* open solder alloy by means of superior strength and compact melting temperature. In this research, a minimal cost lead-liberated solder alloy of Sn-0.7Cu was selected. Elevated energy ball milling method was assumed for the manufacture of nano crystalline solder from this alloy. The milling was conducted for 100 hrs. The milled powders were considered for their crystallite size, changes in morphology as well as decline in its melting temperatures. The outcome reveals that for a milling time of 100 hrs the crystallite size was lessened from 131 nm to 36 nm. *DSC* evaluations reveal a steady transition from pointed exothermic peak in bulk alloy to broad depleted temperature summits at lessened particle sizes. Nano crystalline powder was compacted into billets with a 98% theoretical compaction density. Microwave sintering technology was adopted to sinter these compacted billets. A series of tests like *SEM-EDS*, *XRD*, *DSC*, salt spray fog corrosion studies, density measurements, mechanical properties like hardness, compression, shear and tensile tests were carried out on these solder billets. Results shows that conversion from micro to nano crystalline structure improved mechanical and corrosion resistance was noticed while lowering the melting temperature.

**Keywords:** Pb free solders, High energy ball milling, Nano crystalline materials, Low melting point.

DOI: <http://dx.doi.org/10.4314/ijest.v10i3.2>

### 1. Introduction

In electronic packaging manufacturing, the use of lead-liberated Sn-supported solders is known for quite a few years to get rid of the destructive influences of lead on human's physical condition and the natural world. *Sn-Cu*, *Sn-Ag* and *Sn-Ag-Cu* solders are generally employed lead- liberated solders instead of *Sn-Pb* solders (Turbini et al., 2000). Regrettably, the advanced melting temperature is even now a crucial concern for lead-liberated solders. It is recognized that an advanced melting point brings about an advanced processing temperature that sequentially give rise to advanced defect rates.

With the advancement of lead-liberated solders to be employed in electronic packaging manufacturing, quite a few difficulties are to be encountered. Solder substances participate in vital manners to the reliability of joint assemblies in electronic packaging since they offer mechanical, thermal and electrical stability in electronic assemblage. The continued tendency in the direction of miniaturization and functional density improvement needs extremely lesser solder joints and fine-pitch interlinks for microelectronic packaging in electronic machines. For instance, movable electronic machines like movable computers as well as cell phones, have turned out to be narrower and lesser having extremely complex utilities (Glazer, 1994; Frear et al., 2001; Frear and Subramanian, 2006). The miniaturization of these electronic machines commands superior solder joint reliability. The melting temperature is probably the primary and largely necessary parameter for the expansion of novel solder substances in microelectronic packaging manufacturing.

Sn-3.5Ag and Sn-0.7Cu are one of the largely assuring lead- liberated alloys to replace Pb-Sn solder since it exhibits outstanding mechanical features and enhanced elevated temperature resistance weighed against Pb-Sn solders (Wautelet, 1995; Rani and Murthy, 2013). Bearing in mind the growing cost of silver in the international market, manufacturers of solders are keenly investigating lead- liberated solders devoid of silver, placing the Sn-Cu scheme a targeted option. The eutectic *Sn-Cu* alloy

displays outstanding wettability and is inexpensive in the company of the generally employed solder alloys. In spite of this, its mechanical potency is reasonably low weighed against eutectic *Sn–Pb* and *Sn–Ag–Cu* solders while this could result in reliability concerns.

Several materials, consisting of unadulterated metals, show signs of a modification in properties as their particle sizes move toward nanoscale scope. The growth in the surface-to-volume quotient that takes place obviously as particle sizes get smaller, of necessity augments the comparative ratio of superior energy surface atoms. The influence could comprise a modification in reactivity, modification in electromagnetic characteristics, varying electronic and optical characteristics. Takagi originally examined melting point downturn of quite a few kinds of metal nano particles in the year 1954 (Takagi, 1954). Hence, nano materials are interesting candidates for soldering applications (Maruyama et al., 2008; Yan et al., 2012; Buršik et al., 2012).

From the above and currently available literature it is evident that a little information is available in the direction of lowering the melting temperatures along with increasing strength of existing Sn–0.7 wt. % Cu solder alloy. Hence in the proposed research work is focused to address the above gap; and this revealed information is certainly useful to the soldering industry. In the present work synthesis of micro and nano crystalline Sn-0.7wt%Cu have been prepared by mechanical alloying method with help of high energy ball mill. The milled nano crystalline powder was compacted in 12 X 12 mm diameter solid form by powder metallurgy route and sintered by using microwaves. These eutectic alloys were characterized for its *XRD*, *SEM–EDS* analysis and *DSC* tests; and further characterization like hardness, compression, solder joint strength and also fog corrosion tests were carried out.

## 2. Materials and Methods

In this study powders of *Sn* (-100 mesh purity 99.98wt%, M/s. Alfa Aesar, MA, USA) and *Cu* (30 $\mu$ m, 99.9wt%, M/s. Alfa Aesar, MA, USA) were used as initial materials. The Sn-0.7%Cu solder bulk alloy was prepared via powder metallurgy route. The initial *Sn* & *Cu* powders were calculated based on their wt. % and this mixture was mixed and blended homogeneously in a Retsch, PM 200 ball mill without any balls for a period of 15 minutes. The solder alloy particle size cutback from micron stage to the nano stage was conducted employing an elevated-energy planetary ball mill (Type: Retsch, PM 200, Germany) in a tungsten carbide cavity employing tungsten carbide balls having 10 mm size. The milling operation was conducted at room temperature while the ball-to-powder weight quotient (BPR) was upheld at 10:1 all the way through the process. The speed at rotation was held constant at 300 rpm. Toluene was employed as the means having an anionic surface energetic mediator to keep away from agglomeration. The complete milling period of the grinding down procedure was restricted to 100 hrs while afterward no more substantial drop in particle size were noted. The milled samples were obtained at a space of every 10 h of milling time while being conserved in toluene for additional classification.

The new and milled solder alloy particles were classified by means of an X-Ray Diffractometer (Type: 2036E201; Rigaku, Ultima IV, Japan). JADE software was employed to examine the structural variations and stage transitions of particles that happen in the course of mechanical milling. Specimen grounding of *XRD* was attempted as maintained by typical exercise. The X-ray diffraction evaluations were conducted using a Goniometer type 2036E201 employing *Cu K* radiation ( $K = 1.54056 \text{ \AA}^0$ ) at an accelerating voltage of 40 kV as well as a current of 20 mA. In this examination, the specimen was in a standing situation, merely the arms of the X- ray tube was revolving in the conflicting way up to 90 $^\circ$  of 2 $\theta$  in the course of the examination. The specimens were scanned in the array of 3 $^\circ$  to 90 $^\circ$  of 2 $\theta$  by means of a scan rate of 2 $^\circ$ /min. The examination was conducted to search for the amount of induced strains in the milled solder alloy, its crystallite size and peak height. Scanning electron microscopy (type: SEM – Quanta 400, FEI, Netherlands) was employed to assess the morphological variations noted in the alloy and ball milled powders.

The ball milled Sn-0.7Cu solder alloy powders were uniaxially compressed at a pressure of 510 MPa to billets (12 mm height with 12 mm diameter) in a 1000 ton press. Compressed billets were sintered in Microwave sintering by using a SHARP R-888F domestic microwave oven under ambient atmospheric condition. Microwaves with a frequency of 2.45GHz are generated by a 1.6kW SHARP magnetron (RV-MZA222 2M167B-M32) with an output microwave power of 900W (measured based on the International Electro technical Commission’s standardized method). The cold compacted billets were placed in the center of the inner ceramic plate for sintering. The set time and temperature was 2 min and 160 $^\circ$ C respectively. The situate time included merely heating period and is devoid of holding time to reduce or get rid of mass and/or restricted melting of samples. This approach to heating brings out a largely consistent temperature incline in the samples while it avoids the drawbacks of heating employing traditional heating alone.

The density measurements for both the alloy compacted billets were measured before after sintering by using the Archimedes drainage technique with the subsequent expression:

$$= (m) / ((m-m_1) X_{H_2O}) \quad (1)$$

where  $\rho$  is the density of the alloy, ‘m’ is the mass of the alloy sample in air, ‘m<sub>1</sub>’ is the mass of the same alloy sample in distilled water and ‘ $\rho_{H_2O}$ ’ is the density of distilled water (at 293K) is 998 kg/m<sup>3</sup>.

These cold compacted and sintered billets were distinguished by means of an X-Ray Diffractometer (type: 2036E201; Rigaku, Ultima IV, Japan). JADE software was employed to examine the alloys’ phase establishment. The scanning electron microscopy

(type: SEM – JEOL SEM – JSM 6610LV) by means of EDAX energy dispersive X-ray spectroscopy (EDS) was employed for the appraisal of the changes in morphology noted in the cold compacted as well as sintered nano crystalline Sn-0.7 Cu alloy billets.

DSC studies were carried out to evaluate the melting temperatures for the three types of Sn-0.7 Cu alloy samples i.e. micro alloy, 100 hrs milled alloy powder and compacted and sintered nano crystalline alloy billets. For DSC measurements, NETZSCH DSC 200 F3 MAIA Technology Inc. was used. The sample weight is 7 mg. Heating rate is 10°C /min from 160°C to 300°C. The sample weight is 10 mg at nitrogen atmosphere. Heating rate was 10°C /min from room temperature to 450°C in Aluminum pan with lid pierced and sealed sample crucible.

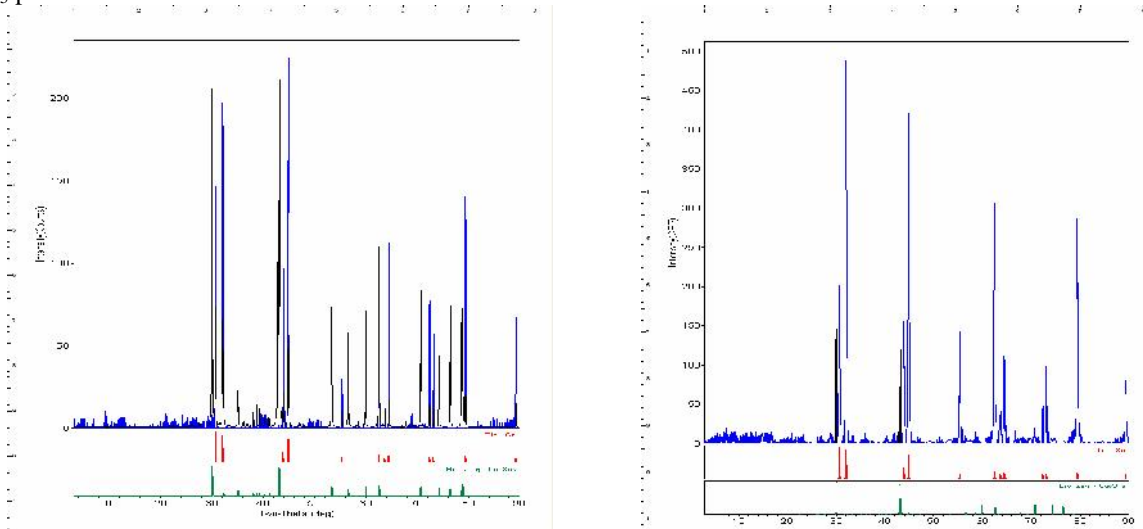
The hardness of the cold compacted and sintered alloy was appraised employing the Leco Vickers hardness analyser (Type: LV 700- USA). The load applied as well as dwell times are 2 kg & 15 sec correspondingly. A mean of ten evaluations were in use for every hardness value. Compression analysis was conducted on cylindrical samples of 12 mm Ø with H/D ratio of 1.0 for both the micro and nano crystalline alloys. Specimens were compacted through inserting them between the flat platens at a steady cross-head speed of 0.5 mm/min in dry situation, employing computer-managed servo hydraulic 10Ton universal testing equipment. Online scheming of load against displacement was made steadily by a data possession scheme.

The solder joint intensity examinations were conducted to appraise the solder joint intensity of both the micro and nano crystalline form of alloy being examined. The samples were arranged in the subsequent manner. Cu plates were structured to create regular substrates of magnitudes 60 X 20 X 1 mm, and these copper plates were scraped by means of 2ml of weak sulphuric acid before the experiment to take away the preliminary oxide scale on the joint specimen located. A rectangular butt joint was afterwards created through fastening the substrates in a custom soldering jig that joins the gap width to 0.5 mm. The micro as well as the lately completed nano-crystalline alloy were employed as a filler material in-between the preset substrates. The solder was repoured, and linkages were created through the placement of the whole soldering assembly (jig attached by means of substrates and solder) in the repoured oven. It was caused to experience a matching temperature outline to that of the massive samples (150 °C preheat temp. and 240 °C peak temp.). Following soldering, the test samples were cautiously detached from the jig while being ground to get rid of any surplus solder in the region of the linkage to join the thickness of the linkage stratum to 1.0 mm. The tensile tests were conducted on these test specimens employing computer-managed servo hydraulic 10Ton universal testing equipment. Online charting of load against elongation was conducted incessantly by a data acquisition scheme. Salt Spray fog corrosion test was carried out on each micro and nano crystalline alloys of Sn-0.7 Cu. The test was continued until either to observe a pit formation on the sample or for a maximum period of 48 hrs. Testing was carried out as per ASTM B117-2009.

**3. Results and Discussion**

*3.1: Crystallite size and Lattice strain of ball milled Sn-0.7Cu alloy powders*

Figure 1 shows the X-ray diffractograms of Sn-0.7Cu alloy for initial and ball milled at various milling times. From this figure it was evident that two major phases namely Sn and Cu<sub>6</sub>Sn<sub>5</sub> were identified for all the milling times; since these two phases were retaining even after the 100 hrs ball milling also. Sn phase exhibits strong peaks at the 2 theta values of 32.121, 30.759, 43.998, 45.002, 62.622 and 79.602; whereas Cu<sub>6</sub>Sn<sub>5</sub> phase exhibits strong peaks at the 2 theta values of 55.460 and 64.700. It was observed that no contamination was entering from either tungsten carbide balls or from tungsten carbide container; and also observed that the intensity of the peaks got reduced and the peak broadening was increasing as the duration of milling increases for both the Sn and Cu<sub>6</sub>Sn<sub>5</sub> phases.



(a) Initial Sn-0.7% Cu alloy

(b) 100 hrs ball milled Sn-0.7% Cu alloy

Figure 1: X-ray diffraction patterns of Sn-0.7Cu alloy at different milling times: (a) initial (b) 100 hrs ball milled condition

The variations in crystalline stages of Sn-0.7 Cu alloy following ball milling were examined by means of broad angle X-ray diffraction investigations. The presence of stress in the materials yields in lattice distortions of crystals; as a result, the diffraction heights of the crystals are widened. The reduction in crystallite size as well the growth of lattice micro-strain was established employing the normal Williamson-hall examination (Williamson and Hall, 1953) that is described by the subsequent expression:

$$\Delta d_{hkl} \cos \theta_{hkl} = (K / t) + 4 \epsilon \sin \theta_{hkl} \tag{2}$$

Here K is the shape factor (0.9),  $\lambda$  is the X-ray wavelength (1.5406),  $\theta_{hkl}$  is the Bragg angle and t is the effective crystallite size normal to the reflecting planes and  $\epsilon$  is the lattice strain. The instrumental broadening corrected line profile breadth,  $\Delta d_{hkl}$  as a complete width at half maximum (FWHM) were computed through origin software rooted in each reflection of 2 $\theta$  subsequent to 100 hours the reflections of Sn, Cu<sub>6</sub>Sn<sub>5</sub> reflections were employed to develop a linear graph of  $\Delta d_{hkl} \cos \theta_{hkl}$  against  $4 \sin \theta_{hkl}$ . Then crystallite size (t) was attained from the cut-off c (i.e.  $c = K / t$ ) and the strain ( $\epsilon$ ) from the slope (i.e.  $m = \epsilon$ ).

Figure 2 shows the variation of the crystallite size and lattice strain as a function of milling time. A steady reduce in crystallite size was observed; and same was decreased from 131 nm to 36 nm for 100hours milling time. The comparative lattice strain was growing by means of growth in the milling period. This lattice strain grew from 0.276 to 0.673 for original and 100 hours milled powder correspondingly. In the course of ball milling the extreme mechanical deformation that happened to the alloy powder shows that way to the production of lattice strains, crystal imperfections and this in addition to the equilibrium between cold welding as well as fracturing operations among the powder particles is probably to influence the organisational amendments in the powder (Suryanarayana, 2001; Archana et al., 2014; Sharma et al., 2015). The evaluation of crystallite size and lattice strain in the mechanically milled powders is extremely necessary as the stage establishment and change features emerge to be significantly depending on them.

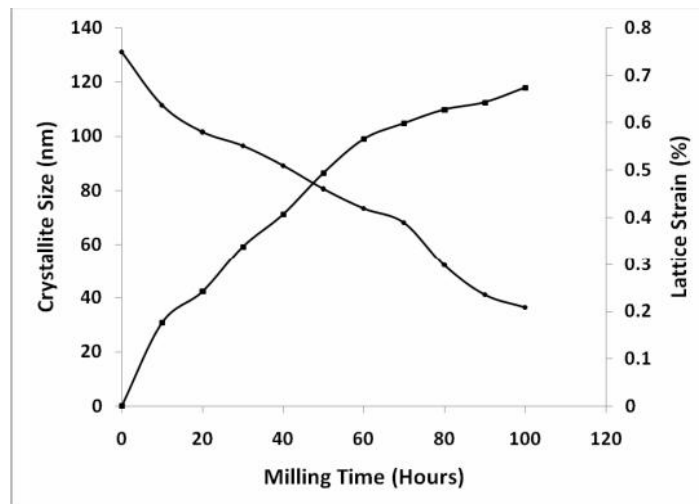


Figure 2: Crystallite size and lattice strain variation with milling time

### 3.2 Compaction, sintering and characterization of milled Sn-0.7Cu Solder alloy powders

A uniaxial hydraulic powder compaction press (1000T) was employed for compaction of this nanocrystalline powder into billets. The results shows 98% theoretical compaction densities were achieved. Microwave sintering technology was adopted to sinter the compacted billets. This technology was enabled to retain the nanocrystalline structure even after sintering process (Nguyen et al., 2014; Tavakol et al., 2015). The average crystallite size of compacted as well as sintered solder alloy billets was analysed from the complete width at half maximum (FWHM) of the X-ray diffraction peak employing the Williamson Hall analysis. Figure 3 exemplifies the disparity of crystalline size before and after cold pressing and sintering of Sn-0.7 Cu nanocrystalline alloy powders. From this figure it was evident that a marginal increase in crystallite size due to combined effects of applied pressure and temperature during pressing and sintering of the alloy powders. The final crystallite size obtained after sintering was 62.97 nm. Decrease in lattice strain was noticed for 100 hrs ball milled followed by compaction & sintering nano crystalline alloy billets; this decrease was 0.7 and 0.033 for before and after sintering respectively. This decrease in lattice strain for sintered alloy compacts might be during sintering operation the stored lattice strains were recovered by the mechanism of recovery, recrystallization and grain growth phenomenon (Dieter, 2013). Figure 4 (a & b) shows the SEM images of Sn-0.7 Cu nanocrystalline alloy before and after sintering process respectively. It shows that no porosity existence; also evidence of uniform compaction and sintering of the solder alloy.

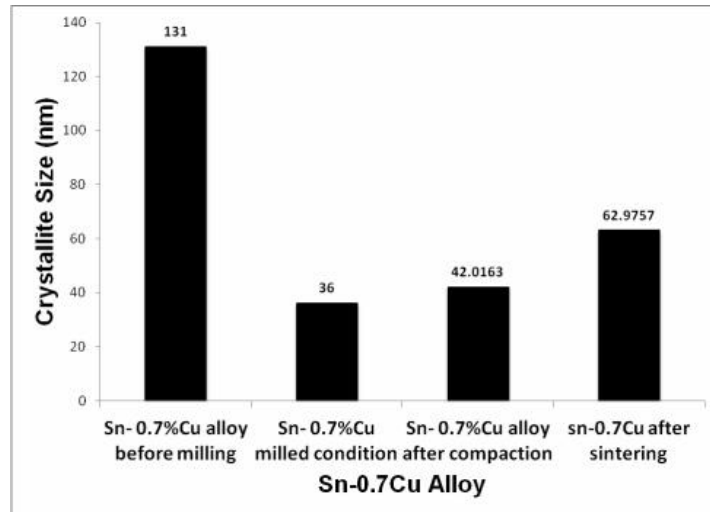


Figure 3: Variation of crystalline size before and after cold pressing and sintering of the Sn-0.7 Cu nanocrystalline alloy powders.

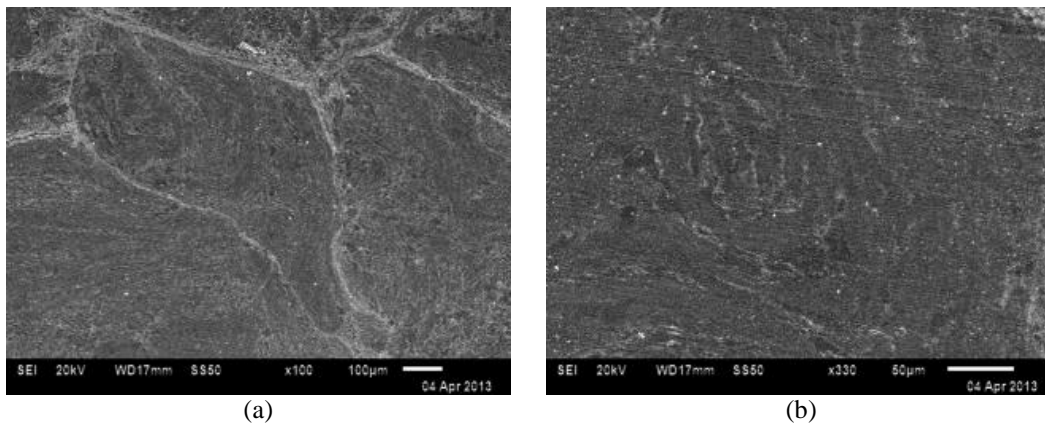


Figure 4: SEM micrographs of compacted solder alloy of Sn-0.7 Cu nanocrystalline alloy (a) Before sintering (b) After sintering process.

The melting properties of the micro and nano crystalline alloys powders as well as compacted and sintered solid samples were analyzed by DSC and the results were shown in Figure 5 (a-c). All these figures exhibit the single exothermic peaks which corresponding to the melting points of the alloy at different processing conditions. The observed melting temperature of Sn-0.7Cu micro alloy was 227.8 °C; this value was identical with the literature values. While increasing the milling time the sharp exothermic peak observed at 227.8 °C in micro alloy steadily expanded and moved to inferior temperatures section. This evidently points to the fact that the surface influences plays a part in sinking the melting temperatures because of the diminishing crystallite sizes, as viewed in the research of Buffat and Borel (1976). The modification in melting temperature ( $T_m$ ) by means of particle size is a surface instigated procedure (Ercolessi et al., 1991; Nanda , 1998; Nanda, 2009; Rao et al., 2013). Variations of melting points with its crystallite size of micro and nano crystalline Sn-0.7 Cu alloy was shown in table 1. The difference in lowering the melting temperature has been observed from micron to nano-sized materials was 37.0°C.

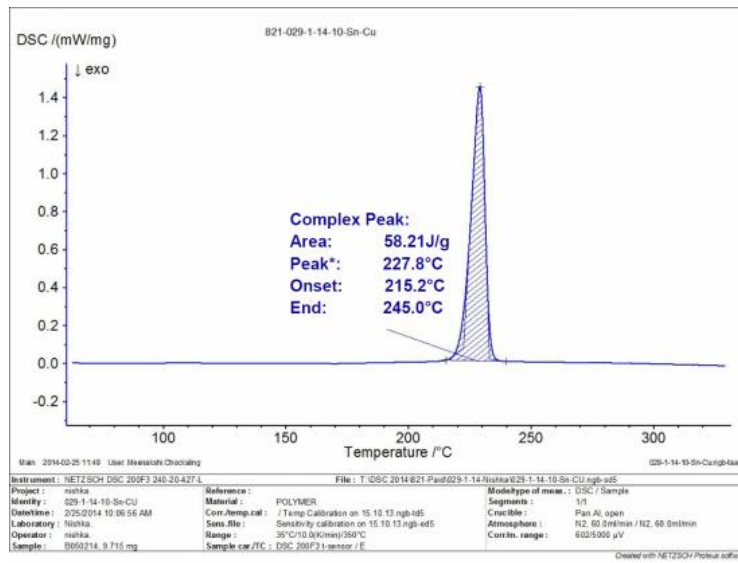


Figure 5(a): DSC curve of micro crystalline Sn-0.7Cu solder alloy

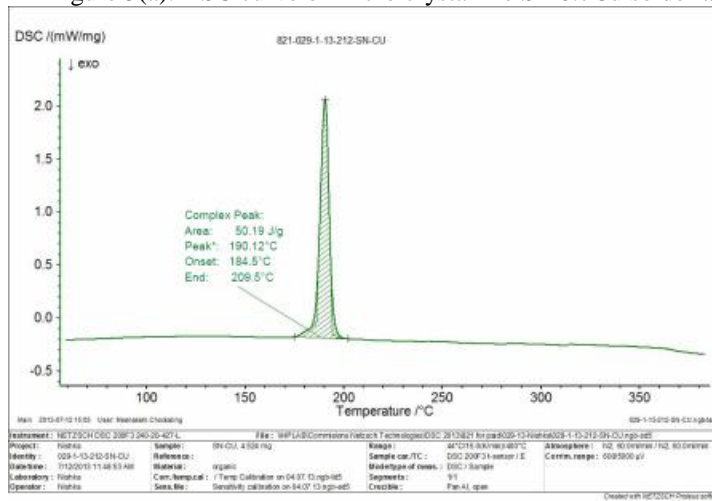


Figure 5(b): DSC curve of nano crystalline Sn-0.7Cu solder alloy after ball milling

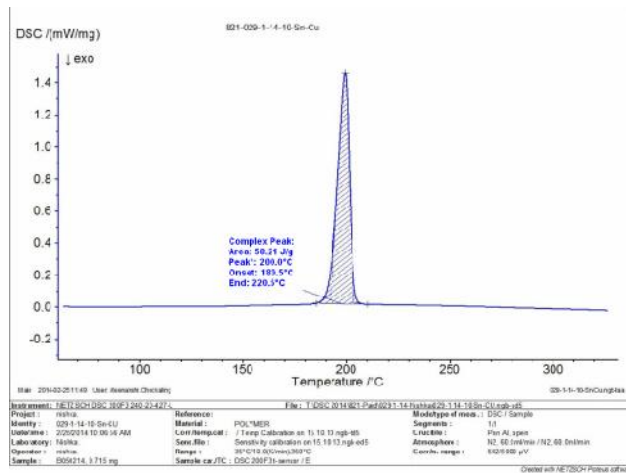


Figure 5(c): DSC curve of sintered sample of Sn-0.7Cu solder alloy

Table 1: Shows the variations of melting points with reference to its crystallite sizes for micro and nano crystalline alloys of Sn-0.7 Cu solder alloy before and after sintering.

S. No	Material	Crystallite size, nm	Melting Temp. °C
Alloy 1	Sn-0.7%Cu micro crystalline alloy	131	227.80
Alloy 2	Sn-0.7%Cu nanocrystalline alloy after ball milled	36	190.12
	microwave sintered Sn-0.7%Cu nanocrystalline alloy	63	200.0

The density measurements for both the micro and nanocrystalline alloy billets were measured before after sintering by using the Archimedes drainage method; the results were revealed in Figure 6. An observable evidence from Figure 6 is the fact that the decrease in density values was observed by converting micron to nanocrystalline size of the same alloy under investigation. Elevated energy ball milling is a severe plastic deformation process, hence during milling more number dislocations might be generated which lead to the decrease in crystal density (Koundinya, 2013).

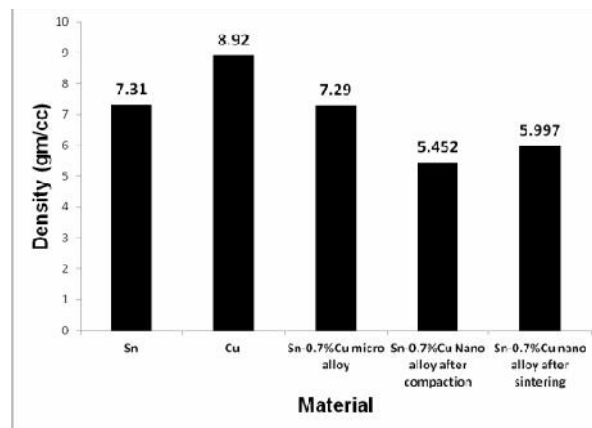


Figure 6: Density variations of Sn-0.7 Cu alloy

### 3.3 Mechanical properties

Figure 7 reveals the comparative hardness profiles of respective pure metals, micro and nano crystalline Sn-0.7Cu alloy. An average of ten observations was made for every hardness value. The obtained hardness values for pure tin, pure copper, Sn-0.7Cu micro and nano crystalline alloy was: 8.5, 40, 14 and 80 VHN respectively. The compression properties of the same alloy for both micro and nano crystalline conditions were obtained by uniaxial compression test. Enhanced strength values were observed for the alloy in nanocrystalline form compare to micro crystalline nature, as shown in Figure 8. Enhanced joint strength was observed for alloy in nanocrystalline form, as shown in figure 9; this might be due to morphological changes associated with refined grain size and reduction in melting temperature of the nanocrystalline alloy.

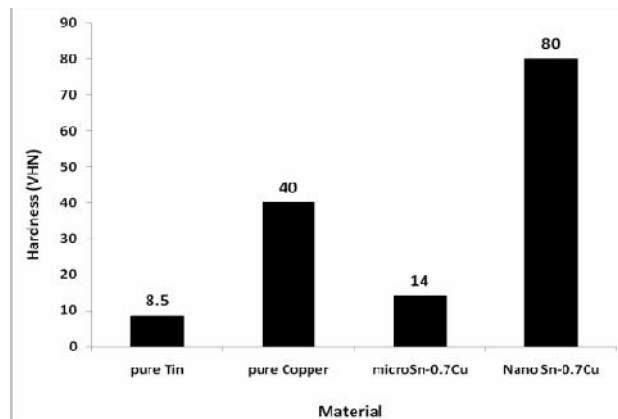


Figure 7: Comparative hardness profiles of respective pure metals, micro crystalline alloy and nanocrystalline alloy.

The enhanced mechanical properties of nano crystalline alloy might be the existence of multiple strengthening mechanisms like: (1) grain boundary strengthening mechanism (while milling the grain size changes for micron to nano crystalline), (2) strain hardening mechanism due to the initiation and duplication of dislocations while milling, and (3) dispersion strengthening of hard copper particulates in the form of intermetallics of  $Cu_6Sn_5$  in soft tin matrix of this Sn-0.7Cu alloy; which is in hard enough nature and also distributed uniformly throughout the soft tin matrix.

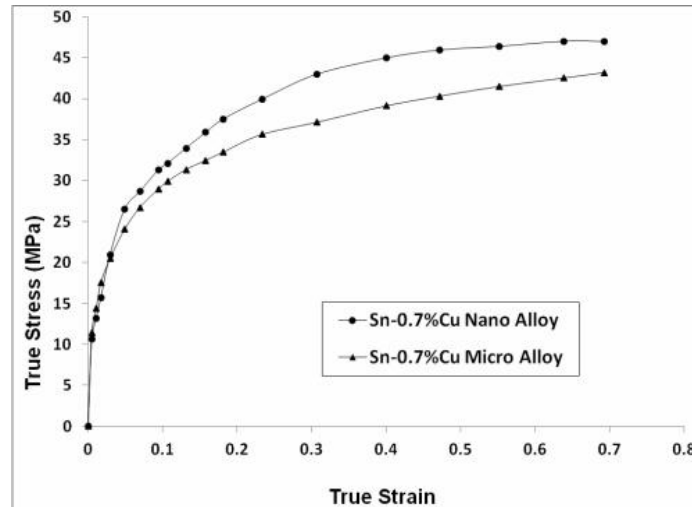


Figure 8: Comparative true stress- true strain curves for Sn-0.7 Cu micro and nanocrystalline alloy.

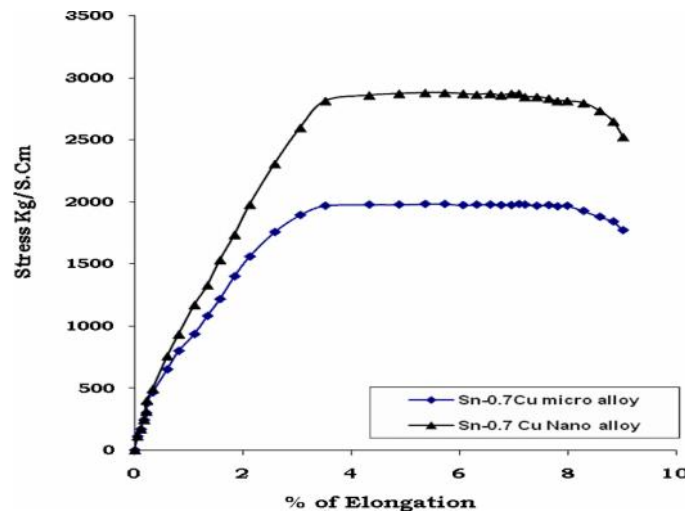


Figure 9: Comparative stress – elongation curves of micro and nano crystalline Sn-0.7Cu alloy.

### 3.4 Corrosion studies

Salt Spray fog corrosion test was carried out on micro and nano crystalline Sn-0.7 Cu alloys. The test was continued until either to observe a pit formation on the sample or for a maximum period of 48 hrs. Testing was carried out as per the ASTM B117-2009; and the process parameters maintained for this was:

- (1) Salt Solution type & water used:  $NaCl$ , reagent grade & distilled Water.
- (2) Chamber Temperature:  $35 \pm 2$  °C,
- (3) Flow Rate: 1.00 ml / hr /  $80 \text{ cm}^2$
- (4)  $NaCl$  Concentration content: 5.10%
- (5)  $pH$  of the Collected Solution: 6.67

The observed results show that no pit or rust formation was noticed for the nanocrystalline solder alloy for the entire test period *i.e.* for a period of 48 hrs. Whereas in case of the same alloy in micro crystalline form; for a period of 24 hrs the test samples color was changed and also multiple pits formation was noticed. This clearly indicates that conversion from micro crystalline to nanocrystalline structure improved corrosion resistance was noticed for the alloy under investigation.

#### 4. Conclusions

1. Mechanical alloying method is an original practicable line of attack to produce super and low cost nanostructured lead-liberated solders for electronic goods.
2. Nanostructured sized Sn-0.7Cu lead-liberated solder alloy were effectively manufactured and examined for their size-reliant melting features.
3. The crystallite size of Sn-0.7Cu alloy lessens from 131 nm 36.28 nm representing a time of 100 hrs milling.
4. A steady conversion from pointed exothermic heights in massive alloy to wide small temperature heights at lessened particle sizes from DSC evaluations reveal an immense latent to alter the melting temperatures of the alloys to the preferred values conditional on the use area.
5. Decreased density values were observed for the alloy while converting from micro to nanocrystalline structure.
6. Enhanced hardness, compression and solder joint strengths were noticed for the alloy in nanocrystalline form.
7. The observed results for salt spray fog corrosion test show that no pit or rust formation was noticed for the nanocrystalline solder alloy during the entire test period i.e. for a period of 48 hrs. Whereas in case of micro crystalline alloy for a period of 24 hrs the test samples color was changed; and also multiple pits formation was noticed.

#### Acknowledgement

One of the authors (Prof. JBR) thank the Department of Science and Technology, New Delhi for their financial support under DST Fast Track Scheme for Young Scientists (*File No: SR/FTP/ETA-104/2010*); and Department of Metallurgical Engineering, Andhra University College of Engineering, Visakhapatnam, India to have offered the essential support to carry out the experiments.

#### References

- Archana M. S., Ramakrishna M., Gundakaram R.C., Srikanth V. V. S. S., Joshi S. V., and Joardar J., 2014, Nanocrystalline phases during mechanically activated processing of an iron (Fe) aluminum (40 at% Al) alloy, *Journal of Materials and Manufacturing Processes*, Vol.29, No. 7, pp.864.
- Buffat Ph, Borel J.P, 1976, Size effect on the melting temperature of gold particles, *Journal of Physical Review A.*, Vol. 13, pp. 2287-2298.
- Buršík, J., Buršíková, V., Pešina, Z., Sopoušek, J., 2012, Mechanical properties and microstructure of model lead-free joints for electronics made with use of nano powders, *Chemické Listy*, Vol.106, pp.390-392.
- Dieter GE, 2013, *Mechanical Metallurgy*, McGraw - Hill Education (India) Pvt Limited, New Delhi, pp.231-236.
- Ercolessi F, Andreeoni W, Tosetti E, 1991, Melting of small gold particles: mechanism and size effects, *Journal of Physical Review Letters*, Vol.66, No. 7, pp.911-914.
- Frear D.R., Subramanian K. N., 2006, Issues related to the implementation of Pb -free electronic solders in consumer electronics, Lead free Electronic Solders, *Journal of Material Science: Materials in Electronics*, pp. 319-330.
- Frear D.R., Jang J.W., Lin J.K, Zhang C., 2001, Pb-free solders for flip-chip interconnects, *The Journal of the Minerals, Metals and Materials Society (TMS)*, Vol. 53, No. 6, pp.28-32.
- Glazer J, 1994, Microstructure and mechanical properties of Pb-free solder alloys for low-cost electronic assembly: A review, *Journal of Electronic Materials*, Vol. 23, No. 8, pp.693-700.
- Koundinya N. T. B. N., Babu CS., Sivaprasad K., Susila P., Babu N.K, Rao JB., 2013, Phase evolution and thermal analysis of nanocrystalline AlCrCuFeNiZn high entropy alloy produced by mechanical alloying, *Journal of Materials Engineering and Performance*, ASM International, Vol. 22, pp.3077-3084.
- Maruyama M, Matsubayashi R, Iwakuro H, Isoda S, Komatsu T, 2008, Silver nanosintering: a lead-free alternative to soldering, *Applied Physics A (Material Science Processing)*, Vol.93, No. 2, pp. 467-470.
- Nanda K.K, 1998, Size-dependent melting of small particles: A classical approach, *European Journal of Physics*, Vol.19, pp.471-472.
- Nanda K K, 2009, Size-dependent melting of nanoparticles: Hundred years of thermodynamic model, *PRAMANA- Journal of Physics*, Indian Academy of Sciences, Vol. 72, No. 4, pp. 617-628.
- Nguyen NT, Nguyen BH, Ba DT, Pham DG, Khai TV, Nguyen LT, and Tran LD, 2014, Microwave-assisted synthesis of silver nanoparticles using chitosan: A novel approach, *Journal of Materials and Manufacturing Processes*, Vol.29, No. 4, pp.418.
- Rao J.B., Kush D, Murthy I.N., 2013, Synthesis and characterization of bulk nano crystalline Pb free solders – 8<sup>th</sup> Pacific Rim International Conference on Advanced Materials and Processing (PRICM-8), August 4-9, Hilton Waikoloa Village, Waikoloa, Hawaii, USA. John Wiley & Sons, Inc. Hoboken, New Jersey, pp. 3237-3246.
- Rani S.D., Murthy G.S., 2013, Evaluation of bulk mechanical properties of selected lead-free solders in tension and in shear, *Journal of Materials Engineering and Performance*, ASM International, Vol.22, No. 8, pp. 2013-2359.

- Sharma P, Sharma S, and Khanduja D, 2015, On the use of ball milling for the production of ceramic powders, *Journal of Materials and Manufacturing Processes*, Vol.30, No. 11, pp. 1370.
- Suryanarayana C., 2001, Mechanical alloying and milling, *Progress in Materials Science*, Vol. 46, No. 1–2, pp.1–184.
- Tavakol M., Mahnama M., and Naghdabadi R., 2015, Mechanisms governing microstructural evolution during consolidation of nanoparticles, *Journal of Materials and Manufacturing Processes*, Vol.30, No. 11, pp.1397.
- Takagi, M., 1954, Electron-diffraction study of liquid-solid transition of thin metal films, *Journal of the Physical Society of Japan*, Vol.9, pp. 359–363
- Turbini LJ, Bent W.R., Ready WJ, 2000, Impact of higher melting lead free solders on the reliability of printed wiring assemblies, *Journal of Surface Mount Technology*, Vol.13, No. 4, pp.10-14.
- Wautelet M, 1995, Size dependent melting of small particles, *European Journal of Physics*, 1995, Vol.16, pp. 283–284
- Williamson GK, Hall WH. 1953, X-ray line broadening from filed aluminum and wolfram, *Acta Metallurgica*, Vol.1, pp. 22–31.
- Yan J, Zou G, Wu A.-P, Ren J, Yan J, Hu A, Zhou Y, 2012, Pressure less bonding process using Ag nanoparticle paste for flexible electronics packaging, *Scripta Materialia.*, Vol.66, No. 8, pp.582-585.

### Biographical notes

**Dr. I Narasimha Murthy** received M. Tech. and Ph.D. from Department of Metallurgical Engineering, Andhra University, Visakhapatnam, in 2011 and 2017 under the guidance of Prof. Babu rao Jinugu. His interest towards the academics and research, he joined in Department of Metallurgical Engineering, AU College of Engineering, Andhra University as a Junior Research Fellow in the year 2012. Presently he is working as teaching assistant in the same department.

**Dr. Babu Rao Jinugu**, working as Professor and chairman board of studies in the Dept. of Metallurgical Engineering, AU College of Engineering, Andhra University, Visakhapatnam since May 2000. He completed his B. Tech and M. Tech in Metallurgical Engineering from NIT Warangal and Ph. D from Andhra University, Visakhapatnam. Prior to join in this University, he worked as Assistant Manager (QA & TD), R&D division of RINL, Visakhapatnam Steel Plant, Visakhapatnam since Sept'1995-April 2000 and also worked as Scientist in C-MET Laboratories, Dept of Electronics, Hyderabad for a period of two months (August - September 1995). He is the Life member for The Indian Institute of Metals (IIM) – Kolkata, Life Member for Tribology Society of India (TSI) and Life member for The Institution of Engineers (IEI). At present he is holding the positions of Joint Secretary - IIM Visakhapatnam Chapter, Chairman - IIM Visakhapatnam Students Chapter and Member- Editorial Board of IIM News Magazine. He is currently working on Development of Pb free nano solders for electronic application under the SERC Fast Track scheme for “Young Scientist” - 2011-2014 (File No. SR/FTP/ETA-104/2010) by Dept of Science and Technology (DST), India and also working for UGC, New Delhi sponsored Major Research Project (File No: 34 -396/2008 (SR) on “Synthesis and Characterization of Al-Fly Ash Nano Composites” and also working for one AICTE, New Delhi sponsored research project (File No: 1-51/FD/CA/ (19)2006-2007) on “Studies on cold workability limits of Aluminium and its alloys”. He was chosen by AICTE-New Delhi as “Career Award for Young Teacher” in the year 2007. He was visited Beijing, China, Singapore and Sydney, Australia in the years 2008 and 2009 respectively for participation and presenting the papers at various international conferences. At present, a total of 125 research papers were published at various national and International journals/ conferences. His current areas of research are Nano Composite Materials and Metal Forming and industrial waste treatments.

**Dr. K Siva Prasad** working as Associate Professor in the Dept of Metallurgical and Materials Engineering, National Institute of Technology, Trichy, Tamil Nadu, India. He obtained his M Tech and Ph D from the Indian Institute of Technology, Madras, Chennai, India. He is author of more than 100 national and international Journals.

Received February 2018

Accepted May 2018

Final acceptance in revised form June 2018